

# Flow in an Elastic Tube Subject to Prescribed Forcing: A Model of Umbilical Venous Flow

S.L. WATERS<sup>a\*</sup> and C. GUIOT<sup>b</sup>

<sup>a</sup>*Department of Applied Mathematics and Theoretical Physics, University of Cambridge, Silver Street, Cambridge, CB3 9EW, UK;*

<sup>b</sup>*Department of Neuroscience and INFM, University of Turin, 10125 Turin, Italy*

*(Received 11 November 2000; Revised 6 July 2001; In final form 26 July 2001)*

We investigate the fluid flow through a finite length, axisymmetric tube when the elastic wall is subject to either a prescribed external pressure or a prescribed motion. The prescribed wall forcing is assumed to consist of a forward travelling wave together with a reflected travelling wave. The dimensionless diameter variation of the tube is taken to be small and perturbation techniques are used to solve the weakly non-linear problem. Particular attention is given to the steady streaming flow that is induced through the non-linear convective acceleration terms. The results are applied to the flow of blood in the umbilical vein (UV), which has important physiological implications.

*Keywords:* Umbilical vein; Steady streaming; Arteries; Fluid flow

## INTRODUCTION

### Physiological Background

The umbilical vessels are a crucial part of the fetoplacental circulation. Deoxygenated blood travels from the foetus to the placenta via the two umbilical arteries and, after the blood has been reoxygenated within the placenta, it returns to the foetus along the single umbilical vein (UV). The diameter of the umbilical arteries is  $\sim 4 \times 10^{-3}$  m and the UV diameter is  $\sim 7 \times 10^{-3}$  m. The umbilical vessels are

enclosed within the umbilical cord and the length of the cord is typically 55–61 cm (Oszukowski, 1998). The flow within the umbilical vessels is driven only by the foetal heart and the foetal heart rate is about twice that of the mothers (Dawes, 1968). Most of the blood exiting the UV passes through the ductus venosus (DV). The DV is a narrow trumpet-like vessel that connects the UV directly with the inferior vena cava and allows the blood to bypass the hepatic circulation.

Two features in particular make the umbilical vasculature unique. Firstly, the umbilical vessels are separated only by a small amount of Wharton's jelly.

---

\*Corresponding author. Present address: School of Mathematical Sciences, University of Nottingham, University Park, Nottingham, NG7 2RD, UK.

This is a gelatinous substance composed of connective tissue cells dispersed in a ground substance consisting of proteoglycans and collagen. The majority of connective tissue cells are myofibroblasts, which have properties intermediate between smooth muscle cells and fibroblasts. The myofibroblasts contribute to the elasticity of the Wharton's jelly by synthesising collagen fibres and participate in the regulation of umbilical flow by virtue of their contractile properties (Takechi *et al.*, 1993). It has been speculated that Wharton's jelly is responsible for regulating the turgor of the cord. This is extremely important for avoiding compression and bending of the cord and thus for ensuring that the blood flows through the cord vessels unimpeded (Nanaev *et al.*, 1997 and references therein). Secondly, the umbilical arteries are twisted in spirals about the single UV and this leads to a high degree of contact between the vessels; see Fig. 1. This helical geometry is established by nine weeks of gestation (Chaurasia and Agarwal, 1979) and the number of twists is thought to be constant throughout pregnancy. During gestation, the cord lengthens by increasing the distance between twists rather than the total number of twists (Benirschke and Driscoll, 1967). The average distance between twists at term is around 2.27 cm (Degani *et al.*, 1995).

Although direct non-invasive measurements of umbilical blood flow can be conducted with Doppler ultrasound, the UV has been studied far less than the umbilical arteries (Willink and Evans, 1995). The foetus is dependent on the supply of oxygen and nutrients from the placenta via the UV and thus the venous blood flow has important clinical implications.

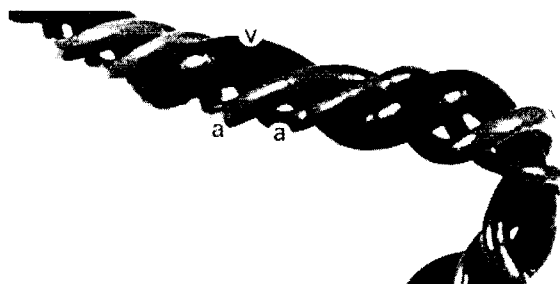


FIGURE 1 The course of umbilical vessels in the umbilical cord. a-umbilical arteries, v-umbilical vein. (Oszukowski, 1998).

For example, the foetus may suffer from Intrauterine Growth Restriction (IUGR) if the quantity of oxygenated blood reaching the foetus is too small (Gill *et al.*, 1984; Ferrazzi *et al.*, 2000). However, if the flow to the foetus is dramatically increased, the foetal heart may become stressed (Kirkpatrick *et al.*, 1976). Furthermore, increased flow may be indicative of Rh-isoimmunisation, antepartum haemorrhage and the presence of pathological placentas (Gill *et al.*, 1984). Finally the presence of UV pulsations during the third trimester of gestation is highly pathological (Nakai *et al.*, 1995). It is important, therefore, to understand how the venous blood flow is regulated in order to maintain an optimum value.

The predominant mechanism that drives the venous blood flow is the mean pressure difference between the two ends of the vessel. However, the venous flow is also subjected to two further influences. Firstly, pressure waves generated in the foetal atria by the periodic contractions of the foetal heart are transmitted to the UV via the ductus venosus (Hellevik *et al.*, 2000). Pulsations in the UV occur most commonly in early pregnancy and in pathological conditions, and are weak compared to the mean venous flow. Secondly, blood flow in the elastic arteries is highly pulsatile and the arteries distend with each pressure pulse (Adamson *et al.*, 1992). Since there exists a high degree of contact between the umbilical vessels, the motion of the arteries will impact on the elastic UV and might be expected to influence the UV flow (Reynolds, 1951; 1978; Lacro *et al.*, 1987; Strong *et al.*, 1993; Degani *et al.*, 1995). We investigate the role of the arterial pressure pulse on the venous flow by developing the following mathematical model.

### Modelling Assumptions

In order to isolate the effect of the umbilical arteries on the venous flow, the mean driving pressure drop along the tube is set equal to zero. In the absence of the arterial pressure pulse the flow is driven by the weak venous pulsations. This is modelled by prescribing the flow rate at the entrance to the tube

(referred to subsequently as the entrance flow rate) and the resulting flow is referred to as the *base* flow. We model the effect of the arterial pressure pulse on this base flow by considering the following two situations.

Firstly, we investigate the hypothesis of Reynolds (1951) that the elastic arteries impose an external pressure on the UV and that this external pressure may enhance venous blood flow (see also Reynolds, 1978). Secondly, if we assume that the Wharton's jelly is essentially incompressible and the umbilical cord is taut then at points at which the arteries distend, the UV diameter would be expected to decrease (in order to conserve the cross-sectional area of the cord).

Thus, we consider the flow of blood in a tube when the elastic wall is subject either to a prescribed external pressure or to a prescribed wall motion. Physiologically, something between the two cases is expected to occur. The flow is driven by the prescribed entrance flow rate and the prescribed wall forcing: these are considered to be of the same magnitude in this model since they are both determined by the pressure waves generated in the foetal heart.

Since the flow of blood in the arteries is pulsatile, and this pulse is reflected at the placenta, we assume the prescribed wall forcing to consist of a forward travelling wave together with a reflected wave. The amplitude of the reflected wave depends on the placental resistance.

The dimensionless diameter variation of the tube is given by  $\epsilon = (R_{\max}^* - R_0^*)/R_0^*$  where  $R_{\max}^*$  is the maximum tube radius and  $R_0^*$  is the mean tube radius. In this analysis, we consider  $\epsilon$  to be small. The governing equations for the fluid flow are non-linear due to the convective acceleration terms and an exact solution cannot be found. However, by exploiting the fact that  $\epsilon \ll 1$  we are able to find an approximate solution for the fluid flow. We consider a small parameter expansion for the dependent variables in powers of  $\epsilon$ . We can then carry out a uniform series expansion of the non-linear governing equations by considering successive orders of  $\epsilon$ . At  $\mathcal{O}(\epsilon)$ , the prescribed forcing will drive a flow which behaves like  $\cos t$ , where  $t$  is the dimensionless time. This is the leading order flow. At  $\mathcal{O}(\epsilon^2)$  the leading-order

flow will interact through the non-linear convective acceleration terms to generate a further flow which consists of an oscillation of twice the fundamental frequency and a mean part (since  $\cos^2 t = (1/2) \times (1 + \cos 2t)$ ). The mean part of the flow is referred to as the steady streaming and we shall concentrate on determining this streaming flow here.

Steady streaming in an elastic tube driven by a purely oscillatory pressure gradient (Womersley, 1955, 1957a,b; Ling and Atabek, 1972) and an oscillatory pressure gradient with nonzero mean (Wang and Tarbell, 1995) has been studied as a model for blood flow in the large arteries. The effect on the steady streaming flow of the phase difference between the pressure gradient and the wall motion has been analysed asymptotically (Wang and Tarbell, 1992) and numerically (Dutta, *et al.*, 1992).

Steady streaming phenomena associated with prescribed motion of the tube wall have also been widely considered. Peristaltic pumping, where fluid is transported by the progression of contraction waves along a distensible tube, has been studied by a number of authors (Fung and Yih, 1968; Shapiro *et al.*, 1969) and a key feature of these problems is the generation of a mean pressure rise along the tube in the absence of a mean flow. The flow in a parallel-sided channel in which one or both the walls oscillate transversely has been examined (Secomb, 1978; Hydon and Pedley, 1993; Hall and Papageorgiou, 1999). Padmanabhan and Pedley (1987) determined the three-dimensional steady streaming in a uniform tube with an oscillating elliptical cross-section. However, none of these authors considered the effect of wave-reflection in their models.

Here, the blood is modelled as a homogeneous, Newtonian fluid and the vein as an isotropic, thin walled, elastic tube of finite length. The vessel pitch is approximately five times greater than the UV diameter and thus as a first approximation we model the UV as a straight tube (see also Kleiner-Assaf *et al.*, 1999). The fluid flow in the tube is governed by the continuity and Navier–Stokes equations together with the no-slip boundary conditions at the tube wall. We determine the fluid flow within the tube and, in particular, we find the mean flow rate along the tube,

that exists in the absence of a mean pressure rise along the tube.

In the next Section the problem is formulated mathematically and the solution for the fluid flow is given and in the following Section results are presented for the mean flow rate generated. The results indicate that, for the parameter regimes considered, the venous flow is not enhanced by the action of the umbilical arteries on the UV. Thus the role of the arterial pressure pulse on the venous flow is likely to be regulatory.

## FORMULATION

We consider an axisymmetric tube as shown in Fig. 2. A cylindrical polar coordinate system  $(r^*, z^*)$  is chosen where  $z^*$  is the coordinate along the axis of the vessel and  $r^*$  is the coordinate in the radial direction. Throughout this paper stars denote dimensional quantities.

The wall of the tube is assumed to be isotropic, thin and elastic. We assume that the walls move along their normal direction and that the wall position is

$$r^* = R_0^* R(z^*, t^*), \quad (2.1)$$

where  $t^*$  denotes time and  $R_0^*$  is the mean tube radius. Here,  $R$  is the (dimensionless) tube radius. The distensibility of the tube wall is  $D^*$  and the tube length

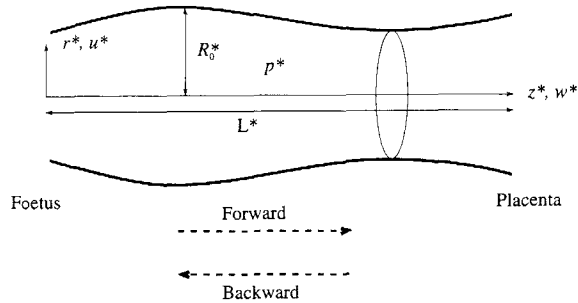


FIGURE 2 Definition sketch. The foetal and placental ends of the vessel are at  $z^* = 0$  and  $z^* = L^*$  respectively. The dashed arrows refer to the direction of the forward and backward travelling waves.

is  $L^*$ . The foetal and placental ends of the vessel are at  $z^* = 0$  and  $z^* = L^*$ , respectively.

The tube contains a homogeneous, incompressible, Newtonian fluid, which has velocity components  $(u^*, w^*)$  and pressure  $p^*$ . The mean fluid pressure (independent of  $z^*$  and  $t^*$ ) is  $p_0^*$ . The kinematic viscosity is denoted by  $\nu^*$ , and  $\rho^*$  is the fluid density.

## Fluid Flow

The fluid flow is governed by the continuity and Navier–Stokes equations. The problem formulation is not straightforward owing to the moving boundary (Eq. (2.1)). To overcome this, we choose a frame of reference in which the tube walls are fixed. We non-dimensionalize as follows so that the wall is now at  $r = 1$ :

$$r^* = R_0^* Rr, \quad z^* = zc^*/\omega^*, \quad t^* = t/\omega^*$$

$$u^* = \omega^* R_0^* u, \quad w^* = c^* w, \quad p^* - p_0^* = \rho^* c^{*2} p, \quad (2.2)$$

where  $\omega^*$  is the angular frequency and  $c^*$  is the wave-speed of the prescribed forcing due to the arterial pressure pulse. Physiologically,  $c^* \approx 5.77 \text{ ms}^{-1}$  (Surat and Adamson, 1997),  $\omega^* \approx 4 \pi \text{ Hz}$  (Guiot *et al.*, 1992) and  $R_0^* \approx 3.5 \times 10^{-3} \text{ m}$  (Oszukowski, 1998) so that  $\omega^* R_0^*/c^* \approx 1 \times 10^{-3}$ . Thus, making the long-wavelength assumption,  $\omega^* R_0^*/c^* \ll 1$ , the dimensionless, governing equations are

continuity:

$$\frac{1}{rR} \frac{\partial}{\partial r} (ru) + \frac{\partial w}{\partial z} - \frac{r}{R} \frac{\partial R}{\partial z} \frac{\partial w}{\partial r} = 0, \quad (2.3a)$$

radial momentum:

$$\frac{\partial p}{\partial r} = 0, \quad (2.3b)$$

and axial momentum:

$$\frac{\partial w}{\partial t} - \frac{r}{R} \frac{\partial R}{\partial t} \frac{\partial w}{\partial r} + \frac{u}{R} \frac{\partial w}{\partial r} + w \left( \frac{\partial w}{\partial z} - \frac{r}{R} \frac{\partial R}{\partial z} \frac{\partial w}{\partial r} \right)$$

$$= - \frac{\partial p}{\partial z} + \frac{1}{\alpha^2 R^2} \frac{1}{r} \frac{\partial}{\partial r} \left( r \frac{\partial w}{\partial r} \right), \quad (2.3c)$$

where  $\alpha = R_0^*(\omega^*/\nu^*)^{1/2}$  is the Womersley parameter and is the dimensionless frequency of the wall motions. Physically,  $\alpha^2$  is the ratio of the frequency of the oscillations to the inverse time-scale for viscous diffusion of momentum. The boundary conditions are

$$w = 0, \quad u = \frac{\partial R}{\partial t} \quad \text{at } r = 1, \quad (2.4a)$$

$$\frac{\partial w}{\partial r} = 0, \quad u = 0 \quad \text{at } r = 0. \quad (2.4b)$$

Equation (2.4a) is the no-slip condition at the tube wall (where the tube wall is at  $r = 1$ ) and condition (2.4b) is the symmetry condition at the tube centre-line. Equation (2.3b) shows that  $p$  is independent of  $r$ . Physiologically,  $R_0^* \approx 3.5 \times 10^{-3}$  m and  $\nu^* = 4 \times 10^{-6}$  m<sup>2</sup>s<sup>-1</sup> so that  $\alpha \approx 6$ ; we thus consider the regime  $\alpha = \mathcal{O}(1)$ .

The dimensionless diameter variation of the tube, given by  $\epsilon$ , is assumed small and we consider a small parameter expansion for the dependent variables in powers of  $\epsilon$  (throughout this paper *c.c.* denotes complex conjugate):

$$\begin{aligned} u(r, z, t) = & \epsilon[u^{[11]}(r, z)e^{it} + c.c.] \\ & + \epsilon^2[(u^{[20]}(r, z) + c.c.) \\ & + (u^{[22]}(r, z)e^{2it} + c.c.)] \end{aligned} \quad (2.5)$$

with similar expansions for  $w$  and  $p$ . The quantities  $u^{[ij]}$  are independent of time and represent the  $j$ th Fourier coefficient of the  $i$ th order term in the expansion of  $u$ . The time-independent terms of  $\mathcal{O}(\epsilon^2)$  represent the steady streaming, which results from the non-linear convective acceleration terms. We also expand the wall radius in powers of  $\epsilon$  as follows

$$R = 1 + \epsilon[R^{[11]}e^{it} + c.c.] + \dots \quad (2.6)$$

Since the steady streaming Reynolds number,  $R_s = \alpha^2 \epsilon^2$ , is much less than unity we can carry out a uniform series expansion of the governing Eqs. (2.3a)–(2.3c) by considering successive orders of  $\epsilon$ .

The leading order,  $\mathcal{O}(\epsilon)$ , solution is

$$\begin{aligned} w^{[11]} &= \frac{i}{2} \frac{\partial f}{\partial z} \left( 1 - \frac{J_0(\sigma r)}{J_0(\sigma)} \right), \\ u^{[11]} &= -\frac{i}{2} \frac{\partial^2 f}{\partial z^2} \left( \frac{r}{2} - \frac{J_1(\sigma r)}{\sigma J_0(\sigma)} \right), \\ \frac{\partial p^{[11]}}{\partial z} &= \frac{1}{2} \frac{\partial f}{\partial z}, \quad R^{[11]} = \frac{-C_1^2}{4} \frac{\partial^2 f}{\partial z^2}, \end{aligned} \quad (2.7)$$

where  $\sigma = e^{3i\pi/4} \alpha$  and  $C_1^2 = 1 - 2J_1(\sigma)/(\sigma J_0(\sigma))$ . The function  $f(z)$  indicates how the flow rate varies with axial position and will be determined subsequently from the axial boundary conditions and the wall behaviour.

In order to determine the steady streaming effects we consider the time-mean governing equations at  $\mathcal{O}(\epsilon^2)$ :

$$\frac{1}{r} \frac{\partial}{\partial r} (ru^{[20]}) + \frac{\partial w^{[20]}}{\partial z} = r \frac{\partial R^{[11]}}{\partial z} \frac{\partial \overline{w^{[11]}}}{\partial r} - R^{[11]} \frac{\partial \overline{w^{[11]}}}{\partial z}, \quad (2.8)$$

$$\begin{aligned} \frac{1}{\alpha^2} \frac{1}{r} \frac{\partial}{\partial r} \left( r \frac{\partial w^{[20]}}{\partial r} \right) &= \frac{\partial p^{[20]}}{\partial z} + \frac{2}{\alpha^2} \frac{R^{[11]}}{r} \times \\ & \frac{\partial}{\partial r} \left( r \frac{\partial \overline{w^{[11]}}}{\partial r} \right) - \left( riR^{[11]} - u^{[11]} \right) \frac{\partial \overline{w^{[11]}}}{\partial r} \\ & + w^{[11]} \frac{\partial \overline{w^{[11]}}}{\partial z}. \end{aligned} \quad (2.9)$$

Here overbars denote complex conjugate. The boundary conditions are

$$\begin{aligned} w^{[20]} = 0, \quad u^{[20]} = 0 \quad \text{at } r = 1, \\ \frac{\partial w^{[20]}}{\partial r} = 0 \quad \text{and } u^{[20]} = 0 \quad \text{at } r = 0. \end{aligned} \quad (2.10)$$

The solution for the steady streaming axial velocity is

$$\begin{aligned}
 w^{[20]} = & \frac{\alpha^2}{4} \frac{\partial p^{[20]}}{\partial z} (r^2 - 1) \\
 & + F(z) \left\{ \frac{-i\alpha^2}{8J_0(\bar{\sigma})\bar{\sigma}} (1 - C_1^2)(rJ_1(\bar{\sigma}r)) \right. \\
 & - J_1(\bar{\sigma}) - \frac{1}{2J_0(\bar{\sigma})} (J_0(\bar{\sigma}r) - J_0(\bar{\sigma})) \\
 & + \frac{1}{4J_0(\sigma)} (J_0(\sigma r) - J_0(\sigma)) - \frac{i\alpha^2}{16} (r^2 - 1) \\
 & \left. - \frac{\bar{\sigma}}{4J_0(\bar{\sigma})J_0(\sigma)} \int_1^r J_0(\sigma r) J_1(\bar{\sigma}r) dr \right\}, \quad (2.11)
 \end{aligned}$$

where  $F(z) = i(\partial^2 f / \partial z^2)(\partial \bar{f} / \partial z)$ . This solution agrees with that in Wang and Tarbell (1995). However the form of  $F(z)$  is different (see Axial dependence section).

We shall determine the mean flow rate in the tube. The flow rate,  $Q$ , is given by the integral of the axial velocity across the cross-section of the tube and in dimensionless terms

$$Q = \int_0^1 w R^2 r dr. \quad (2.12)$$

Substituting the expressions for  $w$  and  $R$  (given by Eqs. (2.5) and (2.6)) and retaining only the terms that are independent of time we get that the mean flow rate is

$$\begin{aligned}
 \mathcal{Q} &= Q^{[20]} + c.c. \\
 &= \int_0^1 (w^{[20]} + 2R^{[11]} \overline{w^{[11]}}) r dr + c.c. \\
 &= \mathcal{Q}(F(z)). \quad (2.13)
 \end{aligned}$$

Thus it remains to determine  $F(z)$ . When  $\mathcal{Q} > 0$  the flow is towards the placenta and the venous flow is reduced. When  $\mathcal{Q} < 0$  the flow is towards the foetus and the venous flow is enhanced.

### Axial Dependence

In the following sections,  $f(z)$  is determined from the axial boundary conditions and the wall behaviour. Since the equations for  $f(z)$  are second order, two axial boundary conditions are required which we take to be as follows:

$$Q^{[11]} = \int_0^1 w^{[11]} r dr = 1 \quad \text{at } z = 0, \quad (2.14a)$$

$$Q^{[11]}|_{z=0} = Q^{[11]}|_{z=2\pi}. \quad (2.14b)$$

Condition (2.14a) prescribes the unsteady entrance flow rate. Condition (2.14b) states that this flow rate is spatially periodic with period equal to the wavelength of the prescribed wall forcing.

### Prescribed External Pressure

We assume a simple linear wall law, since we are considering a physiological situation far from collapse:

$$R = 1 + \frac{k}{2}(p - P_{\text{ext}}), \quad (2.15)$$

where  $k = c^* \rho^* D^*$  and  $P_{\text{ext}}$  is the external pressure given by

$$P_{\text{ext}} = \frac{1}{2} \epsilon [(\phi e^{i\bar{z}} + (1 - \phi) e^{-i\bar{z}}) e^{i\bar{t}} + c.c.] + \dots \quad (2.16)$$

Here,  $\phi$  is the reflection parameter:  $\phi = 0$  corresponds to a forward travelling wave,  $\phi = 0.5$  to a standing wave and  $\phi = 1$  to a reflected travelling wave. Thus as  $\phi$  increases the degree of wave reflection increases. From Eq. (2.7) together with Eq. (2.14) we get that

$$\frac{\partial f}{\partial z} = \tilde{A} e^{i\sqrt{k}z/C_1} - \tilde{B} e^{-i\sqrt{k}z/C_1} + \tilde{C}(\phi e^{i\bar{z}} - (1 - \phi) e^{-i\bar{z}}), \quad (2.17)$$

where

$$\gamma = \frac{2\pi i \sqrt{k}}{C_1}, \quad \tilde{C} = \frac{ik}{k - C_1^2}, \quad \tilde{A} = \tilde{B} \frac{1 - e^{-\gamma}}{1 - e^{\gamma}},$$

$$\tilde{B} = i \left( \frac{4}{C_1^2} + \frac{k}{k - C_1^2} (2\phi - 1) \right) \frac{1 - e^{\gamma}}{e^{-\gamma} - e^{\gamma}}.$$

From the estimates of the stiffness parameter from foetal sheep experiments (Hellevik *et al.*, 1998) the vessel distensibility per unit volume,  $D^* = \mathcal{O}(10^{-4}) \text{ kg}^{-1} \text{ m}^{-1} \text{ s}^2$ . The density of blood,  $\rho^* = \mathcal{O}(10^3) \text{ kg m}^{-3}$  and the wave speed of the prescribed external pressure wave is  $c^* \approx 5 \text{ m s}^{-1}$  from which we get that  $k = c^{*2} \rho^* D^* = \mathcal{O}(1)$ .

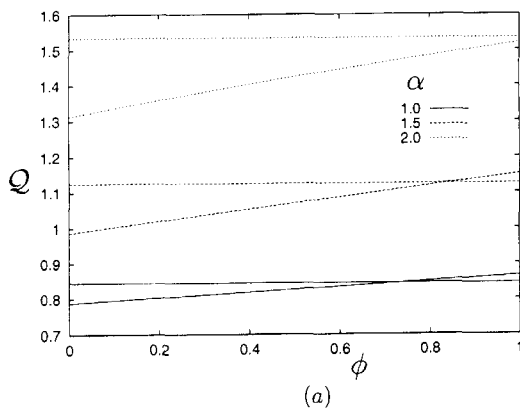
**Prescribed Wall Motion**

Here we impose the following wall motion

$$R^{[11]} = \frac{1}{2} (\phi e^{iz} + (1 - \phi) e^{-iz}) e^{it}, \quad (2.19)$$

where again  $\phi = 0$  corresponds to a forward travelling wave,  $\phi = 0.5$  to a standing wave and  $\phi = 1$  to a backward travelling wave. From Eq. (2.7) together with conditions (2.14) we get that

$$\frac{\partial f}{\partial z} = \frac{2i}{C_1^2} [-1 - 2\phi + \phi e^{iz} - (1 - \phi) e^{-iz}]. \quad (2.20)$$



**RESULTS**

To determine the relationship between the mean flow rate along the tube,  $\mathcal{Q}$ , and the associated mean pressure rise,  $\Pi$ , Eq. (2.13) is integrated with respect to  $z$  between the tube entrance and exit so that

$$\mathcal{Q} = \frac{\lambda^*}{2\pi L^*} \left[ -\alpha^2 \Pi + \int_0^{(2\pi L^*)/\lambda^*} F(z) dz \left\{ \frac{J_1(\bar{\sigma})}{\bar{\sigma} J_0(\bar{\sigma})} \right. \right.$$

$$\times \left[ \left( -\frac{1}{4} + \frac{i\alpha^2}{16} \right) (1 - C_1^2) - \left( \frac{1}{2} + \frac{1}{4} C_1^2 \right) \right]$$

$$\left. + \frac{1}{4} \frac{J_1(\sigma)}{\sigma J_0(\sigma)} + \frac{1}{4} + \frac{i\alpha^2}{64} - \frac{\bar{\sigma}}{4 J_0(\sigma) J_0(\bar{\sigma})} \right.$$

$$\left. \times \int_0^1 r \int_1^r J_0(\sigma r) J_1(\bar{\sigma} r) dr \right\} + c.c. \Big], \quad (3.1)$$

where  $\Pi = (p^{[20]}|_{2\pi L^*/\lambda^*} - p^{[20]}|_0)/16$  and  $\lambda^* = 2\pi c^*/\omega^*$  is the wavelength of the prescribed forcing.

**Prescribed External Pressure**

In Fig. 3, the length of the tube is  $L^* = \lambda^*/2$  and  $k = 1$ . In Fig. 3a, the mean flow rate,  $\mathcal{Q}$ , for zero mean pressure rise ( $\Pi = 0$ ) is plotted as a function of the reflection parameter,  $\phi$ . The horizontal lines correspond to the mean flow rate when there is no

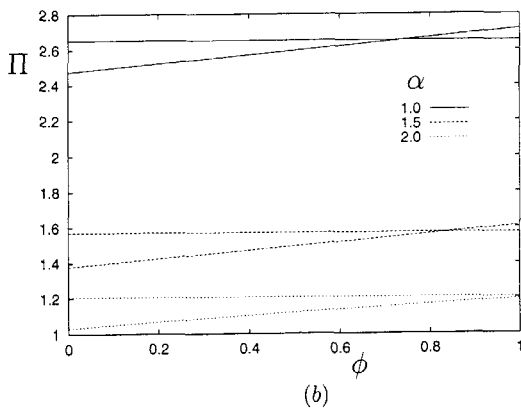


FIGURE 3 (a) Mean flow rate,  $\mathcal{Q}$ , for zero pressure rise as a function of  $\phi$ . (b) Mean pressure rise,  $\Pi$ , for zero flow rate as a function of  $\phi$  ( $\alpha = 1, 1.5, 2, L^* = \lambda^*/2, k = 1$ ). The horizontal lines refer to the case of no external pressure and the lines of positive slope to the case of prescribed external pressure.

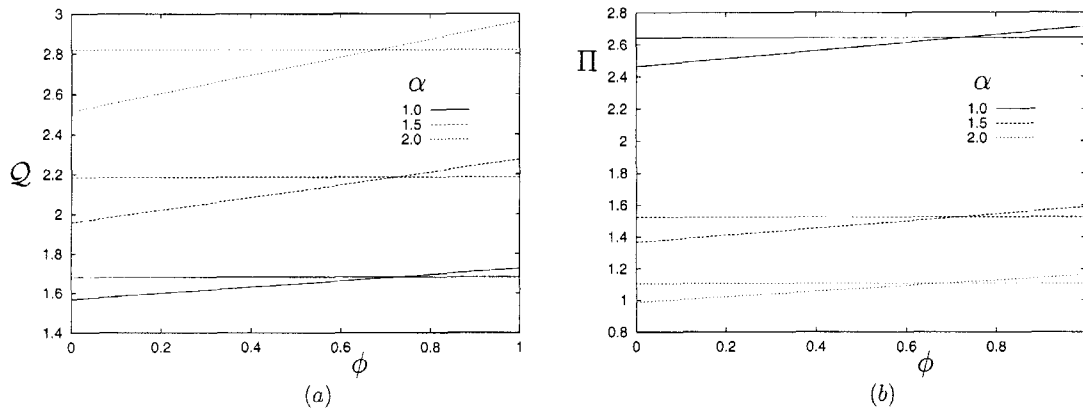


FIGURE 4 (a) Mean flow rate,  $Q$ , for zero pressure rise as a function of  $\phi$ . (b) Mean pressure rise,  $\Pi$ , for zero flow rate as a function of  $\phi$ . ( $\alpha = 1, 1.5, 2, L^* = \lambda^*/4, k = 1$ ).

prescribed external pressure and the flow is driven only by the prescribed entrance flow rate (see also Fung and Yih, 1968; Wang and Tarbell, 1995). The mean flow rate is non-zero (when the mean pressure rise is zero) due to the steady streaming arising from the convective acceleration terms. As  $\alpha$  increases, the mean flow rate increases. The lines of positive slope correspond to the case of prescribed external pressure (Eq. (2.16)). In the presence of external pressure, the mean flow rate increases with the reflection parameter  $\phi$ , so that the flow rate is enhanced by the wave reflection. Physiologically,  $0 < \phi < 0.5$  and in this regime the flow rate is reduced relative to the case where there is no external pressure. Note, however, that for all the values of  $\alpha$  considered, the flow rate is always positive, so that the induced mean flow is towards the placenta and does not enhance venous flow. In Fig. 3b, the mean pressure rise,  $\Pi$ , when the mean flow rate is zero, is plotted as a function of  $\phi$  for several values of  $\alpha$ . Once again, the horizontal lines correspond to the case of no external pressure and the lines of positive slope to the case of prescribed external pressure. As  $\alpha$  increases, the induced mean pressure rise decreases. In the presence of external pressure, the mean pressure rise increases as  $\phi$  increases. In the physiological regime ( $0 < \phi < 0.5$ ), the mean pressure rise is less than the corresponding no external pressure case.

In Fig. 4, the tube length is  $L^* = \lambda^*/4$ . The variation of  $Q$  and  $\Pi$  with  $\alpha$  is as before. However, we see that for the shorter tube the flow rate corresponding to zero mean pressure rise is higher. Moreover, the induced mean pressure rise, for zero mean flow rate, is lower.

Finally, in Fig. 5,  $Q$  and  $\Pi$  are presented for a tube of length  $L^* = \lambda^*/2$ , for various values of  $k$  ( $\alpha = 1$ ). As  $k$  increases, corresponding to the distensibility of the tube wall increasing, the mean flow rate (for  $\Pi = 0$ ) and the mean pressure rise (for  $Q = 0$ ) increase. However, the effect of varying  $k$  on  $Q$  and  $\Pi$  is small compared with the effect of varying  $\alpha$ .

### Prescribed Wall Motion

In this case, if  $R^{11} = 0$  (corresponding to no prescribed wall motion) then  $\partial f / \partial z = \text{const.}$  (see Eq. (2.7)). Hence when the flow is driven purely by the entrance flow rate,  $F(z) = 0$  and no mean flow results. This is in contrast to the previous case of an *elastic* tube where the unsteady entrance flow rate leads to the generation of a mean flow rate via the convective acceleration terms.

In Fig. 6, the tube length is  $L^* = \lambda^*/2$ . Note that here the results are independent of  $k$ . In Fig. 6a,  $Q$  is plotted as a function of  $\phi$  for zero pressure rise. When



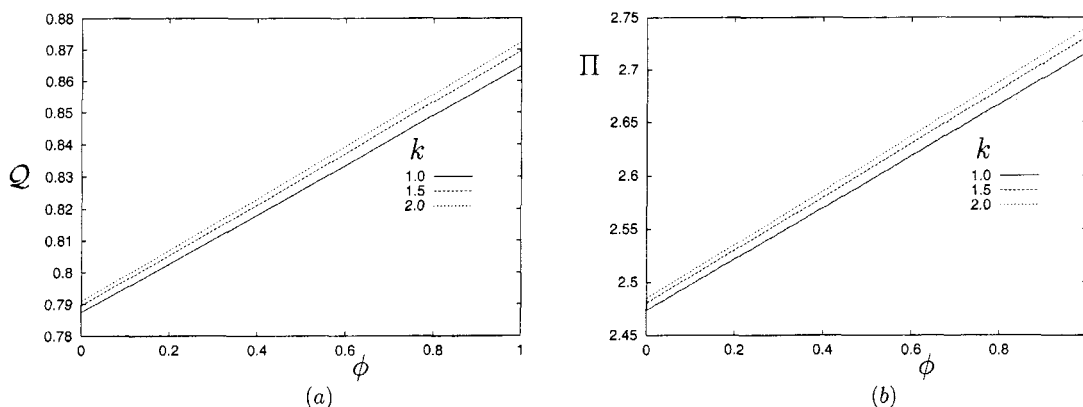


FIGURE 5 (a) Mean flow rate,  $Q$ , for zero pressure rise as a function of  $\phi$ . (b) Mean pressure rise,  $\Pi$ , for zero flow rate as a function of  $\phi$ . ( $k = 1, 1.5, 2, L^* = \lambda^*/2, \alpha = 1$ ).

$\phi = 0.5$ , corresponding to a standing wave, the mean flow rate, in the absence of a mean pressure rise, is zero. When  $0 \leq \phi < 0.5$  (predominantly forward travelling wave)  $Q$  is positive, corresponding to flow in the placental direction. As  $\phi$  increases  $Q$  decreases, so that wave reflection serves to decrease the mean flow rate. When  $0.5 < \phi < 1$  (predominantly negative travelling wave)  $Q$  is negative, corresponding to flow in the foetal direction. As  $\alpha$  increases, the magnitude of the mean flow rate, for a given  $\phi$ , increases. In Fig. 6b, the mean pressure rise,  $\Pi$ , corresponding to zero mean flow rate, is plotted, again as a function of  $\phi$  for several values of  $\alpha$ . For  $\phi = 0.5$ ,

the mean pressure rise is zero. When  $0 \leq \phi < 0.5$  the mean pressure rise is positive, so that the placental end is at a higher pressure than the foetal end. When  $0.5 < \phi \leq 1$  the opposite is true. As  $\alpha$  increases, the magnitude of the pressure rise, for a given  $\phi$ , decreases.

In Fig. 7, the tube is of length  $L^* = \lambda^*/4$ . In Fig. 7a, we see that now when  $\phi = 0.5$ , corresponding to a standing wave, the mean flow rate, for zero mean pressure rise, is positive. This arises since we are now considering a shorter tube. As the tube length increases, the mean pressure drop required to achieve a given mean flow rate increases. Thus, if we fix the

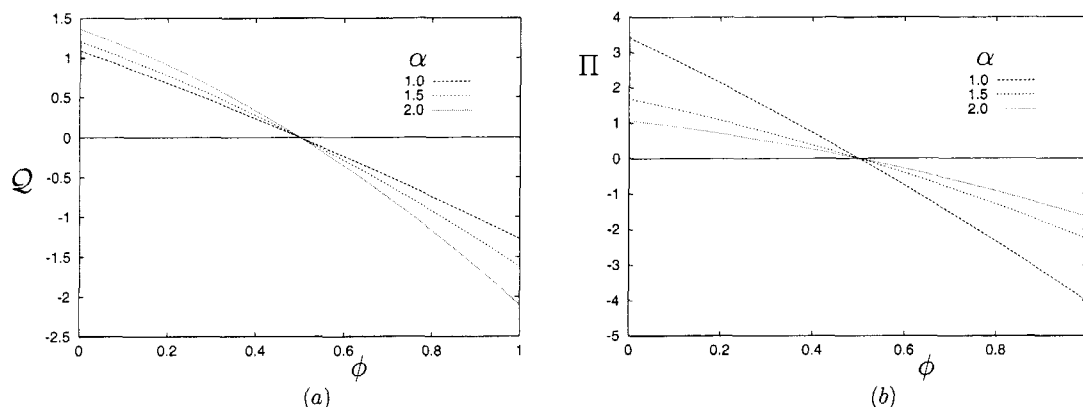


FIGURE 6 (a) Mean flow rate,  $Q$ , for zero pressure rise as a function of  $\phi$ . (b) Mean pressure rise,  $\Pi$ , for zero flow rate as a function of  $\phi$ . ( $\alpha = 1, 1.5, 2, L^* = \lambda^*/2, k = 1$ ).

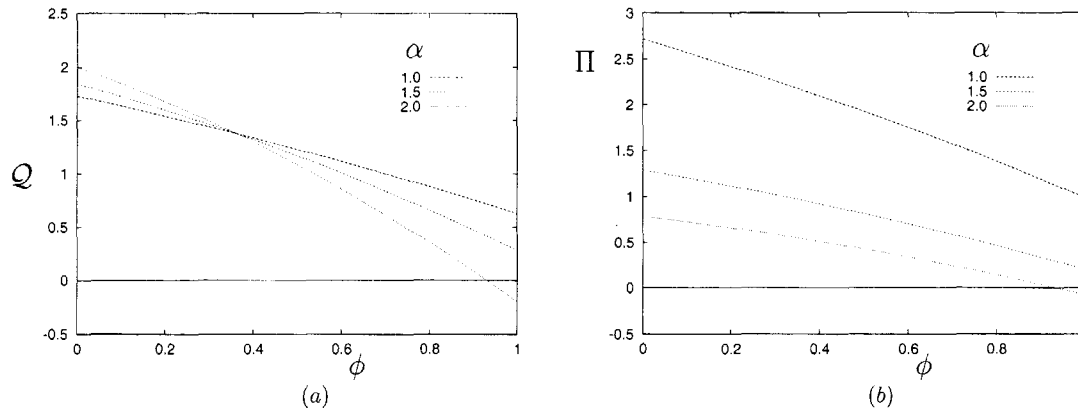


FIGURE 7 Mean flow rate,  $Q$ , for zero pressure rise as a function of  $\phi$ . (b) Mean pressure rise,  $\Pi$ , for zero flow rate as a function of  $\phi$ . ( $\alpha = 1, 1.5, 2$ ,  $L^* = \lambda^*/4$ ,  $k = 1$ ).

pressure rise, the flow rate increases as the tube length shortens. In Fig. 7b, we see that when  $0 < \phi < 0.5$  the pressure rise corresponding to zero mean flow rate is always positive, and as  $\alpha$  increases, the pressure rise decreases.

The critical value of  $\phi$  at which  $Q$  changes from being positive (indicating flow towards the placenta) to being negative (flow towards the foetus) thus depends on vessel length (compare Figs. 6a and 7a). The critical  $\phi$  value also depends on the wavelength  $\lambda^*$  which might be controlled, for example, by varying the wave propagation velocity, which is known to increase in pathological situations of increased placental resistance, such as IUGR (Hill, *et al.*, 1995).

## CONCLUSION

The results of our idealised mathematical model show that a mean flow rate exists in the absence of a mean pressure rise along the tube. This is generated via the non-linear convective acceleration terms. The degree of wave reflection, characterised by  $\phi$ , has a significant effect on the mean flow rate. For the prescribed external pressure case, the mean flow rate is enhanced as the degree of wave reflection increases. In the case of prescribed wall motion, wave reflection leads to a diminishing of mean flow rate. In both

situations, however, increasing  $\alpha$  leads to an increase in the mean flow rate.

The degree of wave reflection depends on the placental resistance. While it is well known that placental resistance increases in IUGR fetuses (Kingdom, *et al.*, 1997), quantitative data determining the effect of increased placental resistance on wave reflection is still lacking. However, physiologically we have that  $0 < \phi < 0.5$  and the mean flow rate (in the absence of a mean pressure rise) is positive. The induced mean flow is in the placental direction so that the venous flow is not enhanced. Thus the action of the arterial pressure pulse on the UV is likely to regulate venous flow rather than enhance it as proposed by Reynolds (1951).

The effects of vessel curvature were neglected in our model so that the model is most appropriate to the conditions of hypo-coiled or non-coiled umbilical cords (Strong *et al.*, 1993). The effect of vessel curvature will be to increase the mean pressure drop required to achieve a given mean flow rate along the vessel (Berger *et al.*, 1983).

The impact of the umbilical arteries on the UV has received significant attention in the medical literature. Studies have suggested that the efficiency of the mechanism proposed by Reynolds could be related to the degree of vessel coiling, which enhances the impact of the umbilical arteries on the UV. It has been suggested that neonates with an absence of normal

umbilical coiling suffer an increased incidence of adverse outcome (Lacro *et al.*, 1987; Strong *et al.*, 1993). Furthermore, Degani *et al.* (1995) proposed that the absence of coiling means that the mechanism put forward by Reynolds (1978) may not be effective. While Reynolds hypothesis is receiving attention in the literature, to date the effect of the arterial pressure pulse on the venous flow has not been investigated. This simple model has shown that in physiological conditions the venous flow is unlikely to be enhanced by the action of the umbilical arteries on the UV, as suggested by Reynolds, but rather the role of the arterial pressure pulse on the venous flow is likely to be regulatory.

#### Acknowledgements

SLW would like to thank her college (Peterhouse) for the award of a research fellowship. The financial support of the visit of CG at DAMTP by the European BIOMED Project (Concerted Action C.BMHA-CT98-3621) is gratefully acknowledged. The authors would also like to thank Dr GM Keith for his careful reading of the manuscript.

#### References

- Adamson, S.L., Whiteley, K.J. and Langille, B.L. (1992) "Pulsatile pressure-flow relations and pulse-wave propagation in the umbilical circulation of fetal sheep", *Circ. Res.* **70**, 761-772.
- Benirschke, K. and Driscoll, S. (1967) *The Pathology of The Human Placenta* (Springer, New York).
- Berger, S.A., Talbot, L. and Yao, L.-S. (1983) "Flow in curved pipes", *Annu. Rev. Fluid Mech.* **15**, 461-512.
- Chaurasia, B.D. and Agarwal, B.M. (1979) "Helical structure of the human umbilical cord", *Acta Anat. (Basel)* **103**, 226-230.
- Dawes, G.S. (1968) *Foetal and Neonatal Physiology* (Year Book Medical, Chicago).
- Degani, S., Lewinsky, R., Berger, H. and Spiegel, D. (1995) "Sonographic estimation of umbilical coiling index and correlation with Doppler flow characteristics", *Obstet. Gynecol.* **86**, 990-993.
- Dutta, A., Wang, D.M. and Tarbell, J.M. (1992) "Numerical analysis of flow in an elastic artery model", *J. Biomech. Engng* **114**, 26-33.
- Hill, A.A., Surat, D.R., Cobbold, R.S.C., Langille, B.L., Mo, L.Y.L. and Adamson, S.L. (1995) "A wave transmission model of the umbilicoplacental circulation based on hemodynamic measurements in the sheep", *Am. J. Physiol.* **38**, R1267-R1278.
- Ferrazzi, E., Rigano, S., Bozzo, M., Bellotti, M., Giovannini, N., Galan, H. and Battaglia, F.C. (2000) "Umbilical vein blood flow in growth-restricted fetuses", *Ultrasound Med. Biol.* **16**, 432-438.
- Fung, Y.C. and Yih, C.S. (1968) "Peristaltic transport", *J. App. Mech.* **35**, 669-675.
- Gill, R.W., Kossoff, G., Warren, P.S. and Garrett, W.J. (1984) "Umbilical venous flow in normal and complicated pregnancy", *Ultrasound Med. Biol.* **10**, 349-363.
- Guiot, C., Pianta, P.G. and Todros, T. (1992) "Modelling the fetoplacental circulation: 1. A distributed network predicting umbilical haemodynamics throughout pregnancy", *Ultrasound Med. Biol.* **18**(6/7), 535-544.
- Hall, P. and Papageorgiou, D.T. (1999) "The onset of chaos in a class of Navier-Stokes solutions", *J. Fluid Mech.* **393**, 59-87.
- Hellevik, L.R., Kiserud, T., Irges, F., Stergiopoulos, N. and Hanson, M. (1998) "Mechanical properties of the fetal ductus venosus and the umbilical vein", *Heart Vessels* **13**, 175-180.
- Hellevik, L.R., Stergiopoulos, N., Kiserud, T., Rabben, S.I., Eik-Nes, S.H. and Irgens, F. (2000) "A mathematical model of umbilical venous pulsation", *J. Biomech.* **33**, 1123-1130.
- Hydon, P.E. and Pedley, T.J. (1993) "Axial dispersion in a channel with oscillating walls", *J. Fluid Mech.* **249**, 535-555.
- Kingdom, J.C.P., Burrell, S.J. and Kaufmann, P. (1997) "Pathology and clinical implications of abnormal umbilical artery Doppler waveforms", *Ultrasound Obstet. Gynecol.* **9**, 271-286.
- Kirkpatrick, S.E., Pitlick, P.T., Naliboff, J. and Friedman, W.F. (1976) "Frank-Starling relationship as an important determinant of fetal cardiac output", *Am. J. Physiol.* **231**, 495-500.
- Kleiner-Assaf, A., Jaffa, A.J. and Elad, D. (1999) "Hemodynamic model for analysis of Doppler ultrasound indexes of umbilical blood flow", *Am. J. Physiol.* **276**, H2204-H2214.
- Lacro, R.V., Jones, K.L. and Benirschke, K. (1987) "The umbilical cord twist: origin, direction and relevance", *Am. J. Obstet. Gynecol.* **157**, 833-838.
- Ling, S.C. and Atabek, H.B. (1972) "A nonlinear analysis of pulsatile flow in arteries", *J. Fluid Mech.* **55**(3), 493-511.
- Nakai, Y., Imanaka, M., Nishio, J. and Ogita, S. (1995) "Umbilical cord venous pulsation in normal fetuses and its incidence after 13 weeks of gestation", *Ultrasound Med. Biol.* **21**(4), 443-446.
- Nanaev, A.K., Kohnen, G., Milovanov, A.P., Domogatsky, S.P. and Kaufmann, P. (1997) "Stromal differentiation and architecture of the human umbilical cord", *Placenta* **18**, 53-64.
- Oszukowski, P. (1998) "Vascularisation of the Human Placenta", *Arch. Perinatal. Med.*
- Padmanabhan, N. and Pedley, T.J. (1987) "Three-dimensional steady streaming in a uniform tube with an oscillating elliptic cross-section", *J. Fluid Mech.* **178**, 325-343.
- Reynolds, S.R.M. (1951) "Arterial and venous pressures in the umbilical cord of sheep and the nature of venous return from the placenta", *Am. J. Physiol.* **166**, 25-36.
- Reynolds, S.R.M. (1978) "Mechanisms of placentofetal blood flow", *Obstet. Gynecol.* **51**(2), 245-249.
- Secomb, T.W. (1978) "Flow in a channel with pulsating walls", *J. Fluid Mech.* **88**(2), 273-288.
- Shapiro, A.H., Jaffrin, M.Y. and Weinberg, S.L. (1969) "Peristaltic pumping with long wavelengths at low Reynolds number", *J. Fluid Mech.* **37**(4), 799-825.
- Strong, T.H., Elliott, J.P. and Radin, T.G. (1993) "Non-coiled umbilical blood vessels: a new marker for the fetus at risk", *Obstet. Gynecol.* **81**, 409-411.
- Surat, D.R. and Adamson, S.L. (1997) "Downstream determinants of pulsatility of the mean velocity waveform in the umbilical artery as predicted by a computer model", *Ultrasound Med. Biol.* **22**(6), 707-717.

- Takechi, K., Kuwabara, Y. and Mizuno, M. (1993) "Ultrastructural and immunohistochemical studies of Wharton's jelly umbilical cord cells", *Placenta* **14**, 235–245.
- Wang, D.M. and Tarbell, J.M. (1992) "Nonlinear analysis of flow in an elastic tube (artery): steady streaming effects", *J. Fluid Mech.* **239**, 341–358.
- Wang, D.M. and Tarbell, J.M. (1995) "Nonlinear analysis of oscillatory flow, with a nonzero mean, in an elastic tube (artery)", *J. Biomech. Engng* **117**, 127–135.
- Willink, R. and Evans, D.H. (1995) "Volumetric flow measurement, by simultaneous Doppler signal and B-mode image processing: a feasibility study", *Ultrasound Med. Biol.* **21**, 481–492.
- Womersley, J.R. (1955) "Oscillatory motion of a viscous liquid in a thin-walled elastic tube-I. The linear approximation for long waves", *Phil. Mag.* **46**(7), 199–221.
- Womersley, J.R. (1957a) "Oscillatory flow in arteries: the constrained elastic tube as a model of arterial flow and pulse transmission", *Phys. Med. Biol.* **2**, 178–187.
- Womersley, J.R. (1957b) "An elastic tube theory of pulse transmission and oscillatory flow in mammalian arteries", *WADC Tech. Report*, 56–614.